Ethylene–Octene Copolymer (Engage)–Clay Nanocomposites: Preparation and Characterization

Madhuchhanda Maiti, Susmita Sadhu, Anil K. Bhowmick

Rubber Technology Center, Indian Institute of Technology, Kharagpur 721302, India

Received 28 February 2005; accepted 1 October 2005
DOI 10.1002/app.23348
Published online in Wiley InterScience (www.interscience.wiley.com).

ABSTRACT: In this work, preparation and properties of nanoclay modified by organic amine (octadecyl amine, a primary amine) and Engage (ethylene–octene copolymer)–clay nanocomposites are reported. The clay and rubber nanocomposites have been characterized with the help of Fourier transform infrared spectroscopy (FTIR), transmission electron microscopy (TEM), and X-ray diffraction (XRD). The X-ray results suggest that the intergallery spacing of pristine clay increases with the incorporation of the amine. The XRD peak observed in the range of 3–10° for the modified clay also disappears in the rubber nanocomposites at low loading. TEM photographs show exfoliation of the clays in the range of 10–30 nm in Engage. In the FTIR spectra of the nanocomposite, there are common peaks for the virgin rubber as well as those for the clay. Excellent improvement in mechanical properties, like tensile strength, elongation at break, and modulus, is observed on incorporation of the nanoclay in Engage. The storage modulus increases, tan δ peak decreases, and the glass transition temperature is shifted to higher temperature. The results could be explained with the help of morphology, dispersion of the nanofiller, and its interaction with the rubber. © 2006 Wiley Periodicals, Inc. J Appl Polym Sci 101: 603–610, 2006

Key words: Engage; nanocomposites; octadecyl amine; sodium montmorillonite; rubber; elastomers

INTRODUCTION

Polymer–clay nanocomposites are a relatively new class of materials with enhanced mechanical, barrier and thermal properties when compared with conventional composites and unfilled polymers. Nanocomposites refer to composites in which one of the components has at least one dimension of about a few nanometers. One of the most promising nanocomposite system would be a hybrid, based on organic polymers and inorganic clay minerals, consisting of layered silicates.

The most commonly used clays are the smectite group minerals, such as montmorillonite (MMT), which belongs to the general family of 2 : 1 layered silicates. MMT is a natural inorganic material, having a general chemical structure $(OH)_4Si_8(Al_{4-x}Mg_x)O_{20}$. The structures consist of two fused silica tetrahedral sheets, sandwiching an edge-shared octahedral sheet of either aluminum or magnesium hydroxide. The silicate layers are coupled through relatively weak dipolar and van der Waals' forces. The chemical structure of MMT and its interaction with polymers is presented in the literature.[1] Generally, a quaternary ammonium based organic surfactant is used to modify the MMT/polymer interactions. The Na^+ residing in the interlayers of sodium MMT (NaMMT) can be replaced by organic cations, such as alkylammonium ions, via an ion-exchange reaction to render the hydrophilic-layered silicate to organophilic. The intercalation of a polymer between MMT sheets depends on the surfactant structure.[2,3] Three types of microstructure can be obtained.[4] MMT and a polymer can form immiscible phases. In the exfoliated system, single sheets of MMT are dispersed in the polymer matrix. Another possibility is when a few polymer chains are intercalated between MMT sheets. The sheets remain relatively close to each other. A basal spacing can still be defined. In addition, agglomeration can be observed.

The first polymer nanocomposite was developed by Toyota Central Research Lab in Japan teamed up with Ube Industries Ltd., a Japanese resin supplier, and consisted of nylon 6 interspersed with layers of MMT, a layered silicate clay.[5] Afterward, reports are available on the polymers like nylon,[5–15] polypropylene,[16–20] polyethylene,[21] etc. In the case of rubber, natural rubber,[22] epoxidised natural rubber,[22] ethylene–vinyl acetate copolymer,[23] acrylic,[24] epoxy,[25] polyurethane,[26] styrene–butadiene rubber (SBR),[27,28] butadiene rubber,[29] acrylonitrile–butadiene rubber,[29] etc. have been used.

Engage (ethylene–octene copolymer) is a comparatively new elastomer introduced by DuPont Dow Elastomers.[30]By bridging the gap between rubber and

Correspondence to: A. K. Bhowmick (anilkb@rtc.iitkgp.ernet.in).

TABLE I
Designation Used for the Clays

Name	Designation
Pristine sodium montmorillonite	UN
Octadecylamine modified sodium montmorillonite	OC

plastic, versatile Engage polymers inspire new design possibilities. The flexibility and mechanical properties of synthetic rubbers combined with the processability of plastics make Engage a great material. Engage polymers can be used as the sole polymer in molded goods, such as toys or household items. Engage has become the modifier of choice for automotive thermoplastic olefinic applications, and is increasingly preferred for all-polyolefin auto interior components and innovative interior designs. It has been used in communication cable jackets and a variety of low- to medium-voltage power cable applications. So, nanocomposites made of this elastomer are worth investigating. From our laboratory, we have reported earlier about the reinforcement of Engage by conventional silica filler.[31] In this work, nanoclay has been modified with octadecyl amine, and the modified clay has been incorporated in Engage. Both the clay and the nanocomposites have been characterized by using X-ray diffraction (XRD) technique, transmission electron microscopy (TEM), and Fourier transform infrared spectroscopy (FTIR). The mechanical and dynamic mechanical properties have been measured and correlated with the structure of the nanocomposites.

MATERIALS AND EXPERIMENTAL METHODS

Materials used

The general purpose polyolefin elastomer, Engage 8150 (comonomer octene content is 25 wt %, ML 1 + 4 at 121°C: 35), was kindly provided by DuPont-Dow Elastomers, Wilmington, DE. NaMMT was generously supplied by Southern Clay Products, Gonzales, USA. Its cation exchange capacity was 90 mequiv/100 g. Octadecyl amine, $C_{18}H_{37}NH_2$, was supplied by Sigma Chemical Co., St. Louis, MO. Toluene (analytical grade) was procured from Nice Chemicals Pvt. Ltd., Cochin, India. Ethyl alcohol was supplied by Bengal Chemicals and Pharmaceuticals, Kolkata, India.

Methods

Preparation of modified clay

The clay was modified with octadecyl amine (primary amine). Five grams of clay was mixed with 400 mL of water, and stirred thoroughly at 80°C for half an hour. Octadecyl amine (2.5 g) was melted at 50°C, mixed with conc. HCl (5 mL), and stirred for a few minutes with addition of 200 mL of water. This solution was then mixed with the clay dispersion slowly, with constant stirring, to obtain the modified clay. This modified clay was then filtered and washed thoroughly until it was free of chloride ion (tested with silver nitrate solution). Then, it was dried in a vacuum oven at room temperature (30°C). Table I reports various clays used for the work and their designation.

Preparation of rubber–clay nanocomposite

Ten grams of rubber was dissolved in 100 mL of toluene at 60°C with stirring. One gram of clay was dispersed in 10 mL of ethyl alcohol. Then, it was added to the rubber solution (to remove slight turbidity a little amount of toluene was added) and thoroughly stirred at 2000 rpm for 3 h at 60°C temperature in a mechanical stirrer (Remi Motors Ltd., Mumbai, India), to make a homogeneous mixture, which was then cast on a smooth aluminum plate and kept in air, followed by vacuum treatment for 24 h to drive off the solvent.

Table II reports various compositions prepared for this investigation and their designation.

Experimental

X-ray diffraction studies

For characterization of the clays and the rubber composites, XRD studies were performed using a PHILIPS X-PERT PRO diffractometer in the range of 2–9° (2θ) and Cu-target ($\lambda = 0.154$ nm). Then, d-spacing of the clay particles was calculated using the Bragg's law. The samples were placed vertically in front of the X-ray source. The detector was moving at an angle of 2θ, while the sample was moving at an angle of θ.

Fourier transform infrared spectroscopy

NICOLET NEXUS FTIR in diffuse reflectance infrared Fourier transform mode was used within the range of 4000–600 cm^{-1} for the characterization of the powder clay samples. FTIR in ATR mode, using 450 KRS5 prisms at room temperature, was used for the rubber

TABLE II
Formulations for Rubber–Clay Composites and Their Designation

Formulation	Designation
Gum Engage	EN
Engage + 4 phr UN	ENUN4
Engage + 2 phr OC	ENOC2
Engage + 4 phr OC	ENOC4
Engage + 8 phr OC	ENOC8

composites. The samples were scanned from 4000 to 650 cm^{-1} with a resolution of 4 cm^{-1}. All the spectra were taken after an average of 32 scans for each specimen. The results were analyzed using OMNIC software, version 5.1, attached to the spectrophotometer.

Transmission electron microscopy

The samples for TEM analysis were prepared by ultra cryomicrotomy. Freshly sharpened glass knives with a cutting edge of 45° were used to get the cryosections of 50 nm thickness. Since these samples were elastomeric in nature, the sample temperature during ultra cryomicrotomy was kept constant at −130°C (which was well below the glass transition temperature, [T_g]), at which the samples existed in a hard glassy state, thus facilitating ultra cryomicrotomy. The cryosections were collected and directly supported on a copper grid of 200-mesh size. The microscopy was performed using PHILIPS (model no. CM 12) electron microscope, operating at an accelerating voltage of 120 kV.

Mechanical properties

Tensile specimens were punched out from the cast sheets, using ASTM Die - C. The tests were carried out as per the ASTM D 412–98 method in a Universal Testing Machine (Zwick 1445), at a crosshead speed of 500 mm/min at 25°C. The average of the three tests was reported here.

Dynamic mechanical thermal analysis

The dynamic mechanical spectra of the blends were obtained by using a dynamic mechanical thermal analyzer (DMTA) IV, (Rheometric Scientific, Piscataway, NJ). The sample specimens were analyzed in tensile mode at a constant frequency of 1 Hz, with a strain of 0.01%, and a temperature range from −80 to 80°C at a heating rate of 2°C/min. The data were analyzed by RSI Orchestrator application software on an ACER computer attached to the machine. Storage modulus (E'), loss modulus (E''), and loss tangent (tan δ) were measured as a function of temperature for all the samples under identical conditions. The temperature corresponding to the peak in tan δ versus temperature plot was taken as the glass–rubber transition temperature (T_g).

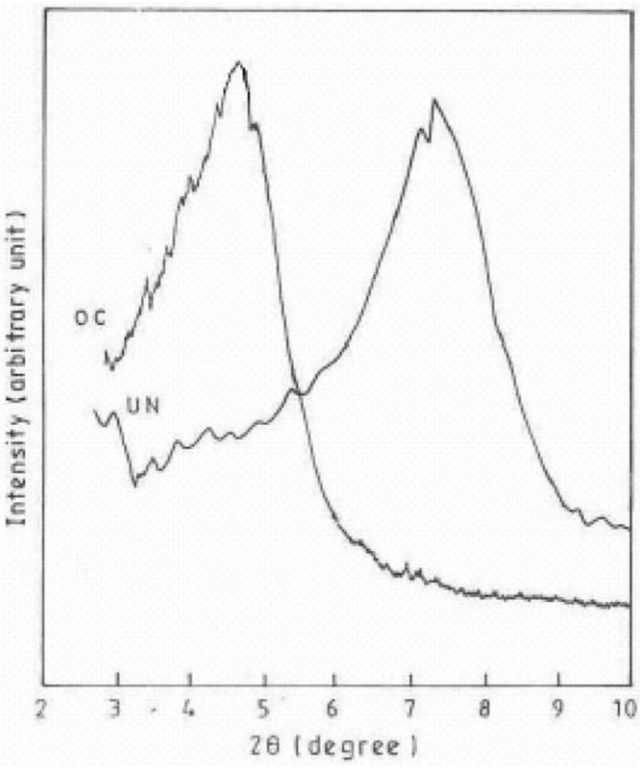

(a)

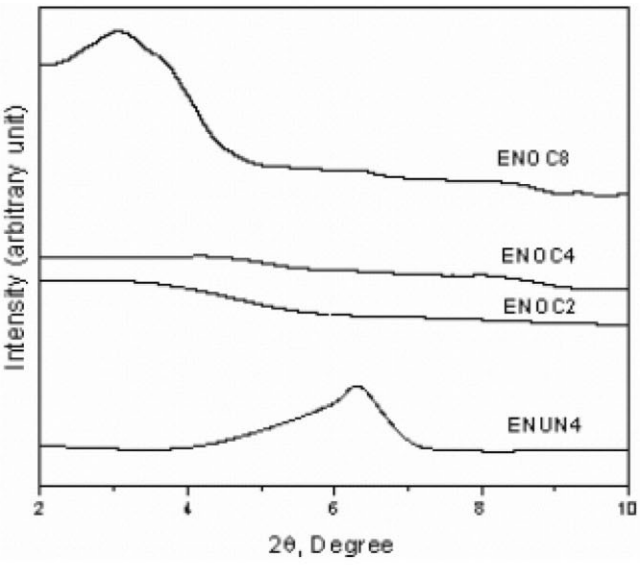

(b)

Figure 1 (a) XRD of UN and OC; (b) XRD of different nanocomposites.

RESULTS AND DISCUSSION

X-ray diffraction

The X-ray diffractograms of the unmodified and the modified clays and their nanocomposites are shown in Figures 1(a) and 1(b). The intergallery spacings of different clays and nanocomposite are tabulated in Table III. In the case of pristine NaMMT, the peak 2θ value is at 7.4°, and the corresponding d-spacing value is 1.19 nm. Similarly, for the modified clay, OC, there is peak at 2θ value of 4.7°. This corresponds to the d-spacing value of 1.88 nm. It indicates that there is a 58% increment observed in the case of OC. In other words, intergallery spacing expands in the case of

TABLE III
Gallery Spacings of Different Clays and Nanocomposites

Sample no.	2θ (degrees)	Gallery gap (nm)
UN	7.4	1.19
OC	4.7	1.88
ENUN4	6.2	1.43
ENOC2	No peak	—
ENOC4	No peak	—
ENOC8	3.1	2.85

modified clay. The increase is due to the incorporation of the ammonium cation within the gallery of clay layers, as explained in earlier papers.[6–13]

In the case of ENUN4, there is a peak at 6.2°, corresponding to the *d*-spacing of 1.43 nm, which is higher than that of unmodified clay, UN. It indicates intercalation of polymers into the clay, UN. Here the polymer–clay interaction is much lower, as the clay is hydrophilic in nature and the polymer is an organic one. A similar observation is made with SBR.[27]

On the other hand, there is no peak in the XRD of ENOC2 and ENOC4. This indicates total exfoliation of the layered clay structure. Exfoliation of the layered structure of nanosilicates occurs on mixing the modified clay with the rubber solution followed by evaporation of solvents. This exfoliation may be attributed to the nonpolar–nonpolar interaction between the aliphatic chain of amine and the nonpolar rubber matrix. However, intercalation is observed in the case of ENOC8. There is a peak at 3.1°, corresponding to the *d*-spacing of 2.85 nm. This may be due to the filler agglomeration at higher filler loading. We have observed exfoliation of the clay in SBR earlier. There are also examples of clay exfoliation in polymers like nylon-6[5] and polypropylene.[20]

FTIR spectroscopy

The FTIR spectra of all the clays and the rubber nanocomposites are compared in Figures 2(a) and 2(b). The characteristic peaks for UN are as follows: around 3635 cm^{-1} for OH, 1640 cm^{-1} for OH bending, 1044 cm^{-1} for Si—O—Si group. On amine modification of UN, there are some extra peaks at around 2928 and 2846 cm^{-1} due to CH_2 stretching frequency, 1865 cm^{-1} due to N^+—H stretching frequency, 1553 cm^{-1} due to N^+—H bending, in addition to the UN peaks. This proves the intercalation of long chain alkyl amines into the gallery gap of the clays.

From FTIR studies, it has been found that EN is a saturated copolymer, since it does not have any peak at 950–965 cm^{-1} (as peaks in the aforementioned region indicate the presence of unsaturation in the compound).

In the nanocomposite, ENOC4, there are two extra peaks along with those of the peaks of EN at 1550 and 1035 cm^{-1}. The former one is due to N^+—H bending, and the latter one due to Si—O—Si group present in the modified clay. Since both the peaks of EN and OC are present in the FTIR of ENOC4, clay is incorporated in the rubber matrix. There is however no shifting of the peaks of ethylene–octene copolymer.

Transmission electron microscopy

TEM pictures are shown in Figures 3(a) and 3(b). The unmodified clay, UN, and the modified clay, OC, show an average particle size of 54 and 28 nm,[27] respectively. The modified clay shows higher structure and lower particle size, that is, high active surface area when compared with the unmodified clay.[27] In the nanocomposite with the unmodified clay, ENUN4, the clay particles are in agglomerated form [Fig. 3(a)]. The average particle size is ~60 nm, and the particles have low aspect ratio. In the nanocomposite with the modified clay, ENOC4, it can be seen that the clay particles are having platelet-like layer structures. The average particle width is ~13 nm. From the above results, it is clear that the polymer-filler interaction is better in the modified clay, and the layered structure is partially exfoliated to give nanoparticles.

Mechanical properties

Mechanical properties of the rubber containing various clays and different filler loadings are given in Table IV and in Figures 4(a) and 4(b). The stress increases with strain linearly in the initial stage as usual, and then increases gradually before a sharp upturn, showing elastomeric nature. The stress–strain curve of ENOC4 lies above those of ENUN4 and EN. This indicates that the modified clay displays increased modulus and ultimate stress over the control.

The modulus (at 100% elongation) values of EN, ENUN4, and ENOC4 are 1.68, 1.78, and 2.73 MPa, respectively. This means that the modulus (at 100% elongation) remains almost unchanged with the addition of UN, but increases about 63% for ENOC4. Increasing the modulus in the case of modified clay is due to better polymer-filler interaction and dispersion. In the case of UN, the polymer and the clay phases are immiscible; hence, there is some agglomeration and nonuniform distribution, as observed in the TEM, which is the reason for the reduced modulus value.

The tensile strength value of EN, ENUN4, and ENOC4 are 9.4, 9.4, and 13.2 MPa, respectively. This means that the tensile strength remains unaltered with the addition of UN. The strength increases about 40% in ENOC4. The tensile strength depends on rubber-filler interaction. As the UN is a hydrophilic one, it is

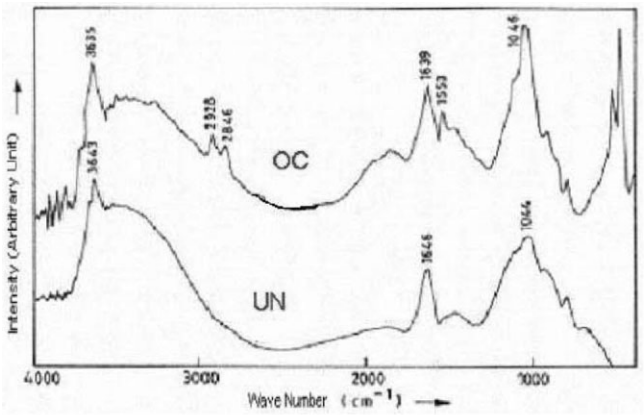

(a)

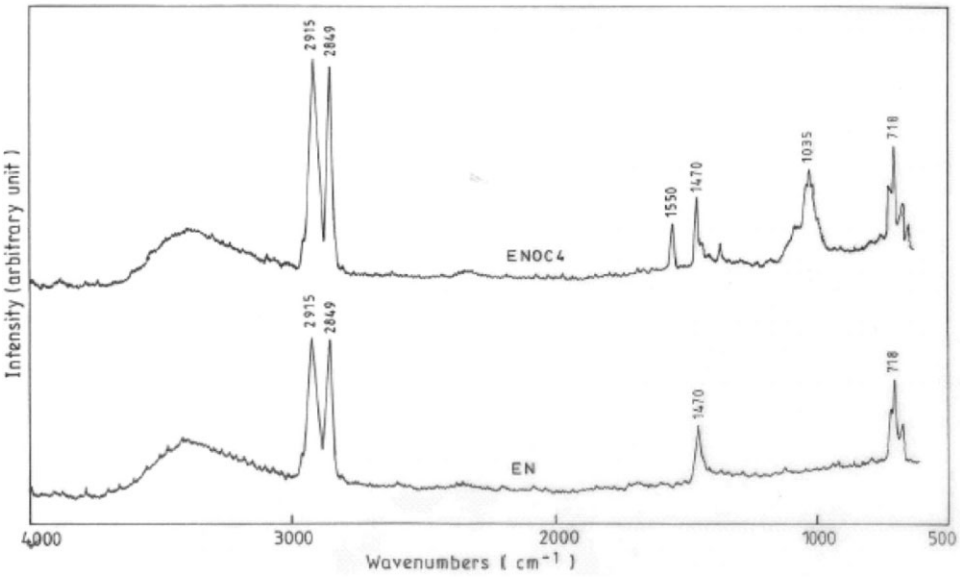

(b)

Figure 2 (a) FTIR spectra of UN and OC; (b) FTIR spectra of EN and ENOC4.

immiscible with organic rubber phase; hence, there is not much interaction with the organic rubber matrix. The increment with the addition of OC is due to the nonpolar–nonpolar interaction and better compatibility between the long alkyl chain of amine and the rubber matrix. The alkyl chain has some structural similarity with the completely saturated structure of EN. The interaction between the OC and the rubber is much stronger, as also revealed by the dynamic mechanical properties discussed later.

The values of elongation at break of EN, ENUN4, and ENOC4 are 920, 935, and 1180%, respectively. Though there is no significant increment in the case of ENUN4, there is an increment of 28% with the addition of OC. The elongation at break values are in accord with the modulus values.

The tensile strength values of ENOC2, ENOC4, and ENOC8 are 9.6, 13.2, and 9.8 MPa. Hence, tensile strength increases with filler loading up to 4 phr, and then decreases [Fig. 4(b)]. This may be due to the agglomeration at higher filler loading (supported by XRD). The elongation at break initially increases upto 2 phr and then decreases with filler loading, but modulus increases gradually with the filler loading, as expected.

Dynamic mechanical thermal analysis

The values of storage modulus and tan δ against temperatures are shown in Figures 5(a) and 5(b). The glass transition temperatures, the tan δ, and the storage moduli at 25°C and at 70°C of different composites are listed in Table V. There is an increase in storage modulus in the glassy region in the case of ENUN4 and ENOC4 when compared with that of EN. Above the $T_{g,}$ there is an increase in storage modulus with all the

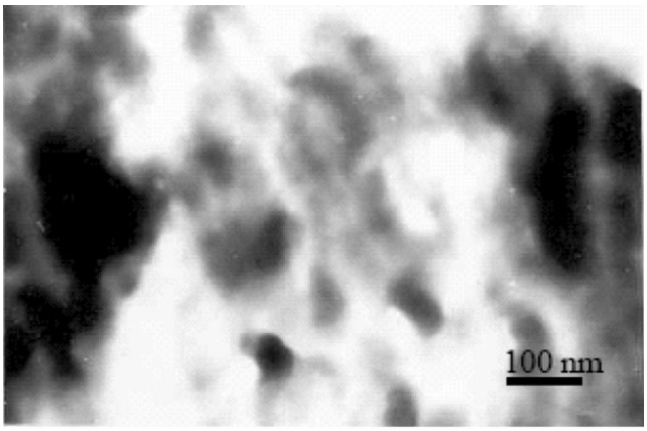

(a)

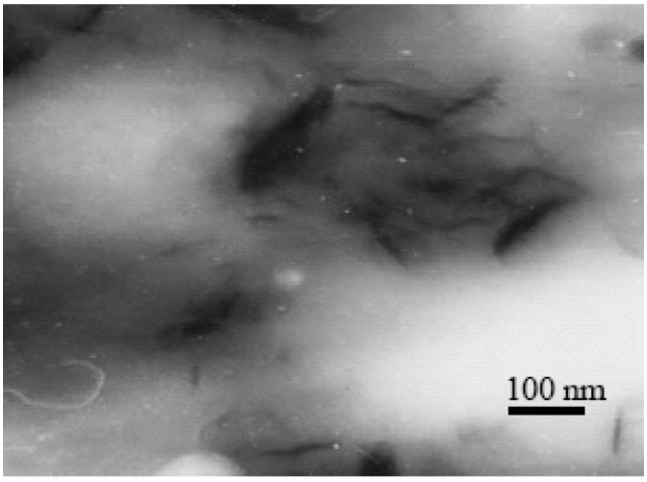

(b)

Figure 3 (a) TEM picture of ENUN4; (b) TEM picture of ENOC4.

clays. The increment is much more in the case of ENOC4 than in ENUN4.This is possible due to better interaction between the modified clay and the rubber matrix. There is another transition at higher temperature; this may be due to melting of the crystallites, which is a characteristic of Engage that has 10% crystallinity.[31]

TABLE IV
Mechanical Properties of Different Nanocomposites

Sample no.	Modulus at elongations (MPa) 100%	200%	300%	Tensile strength (MPa)	Elongation at break (%)
EN	1.68	2.43	2.98	9.4	920
ENUN4	1.78	2.29	2.81	9.4	935
ENOC2	2.55	3.04	3.49	9.6	1230
ENOC4	2.73	3.17	3.55	13.2	1180
ENOC8	2.75	3.06	3.47	9.8	1106

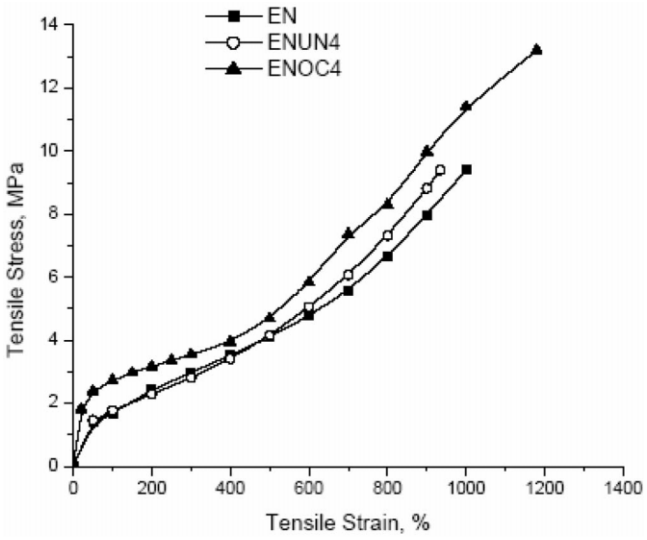

(a)

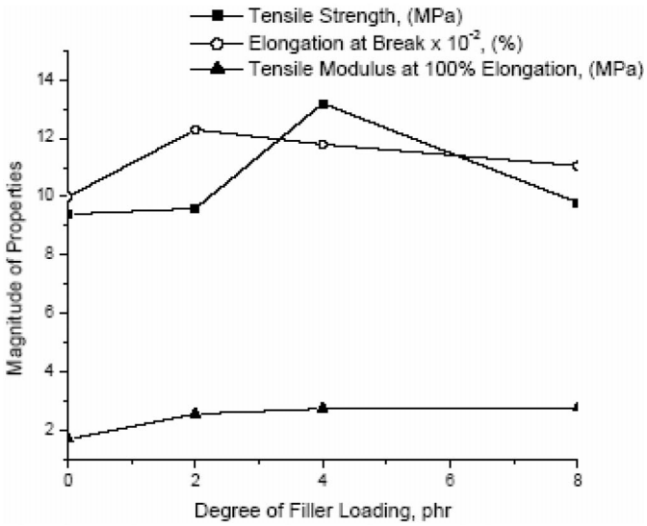

(b)

Figure 4 (a) Tensile stress–strain curve of EN with different clays; (b) Plot of tensile strength, elongation at break, and modulus versus filler loading.

The T_g has been shifted toward higher temperature in ENOC4, though there is no change in the case of ENUN4. This may be due to increased polymer-filler interaction in the case of the modified clay.

The tan δ_{max} decreases slightly, and also the peak broadens in the case of ENOC4 [Fig. 5(b)]. It is known that the height of the dynamic transition of a component of a composite apparently reflects the relative quantity of the component itself. The decrease of tan δ_{max} is the result of a reduction of the relative quantity of bulk rubber "active" in the dynamic transition.[32] As the rubber-filler interaction increases, the available free-chains decreases, resulting in a decrease in tan $\delta_{max.}$ So, decrease in tan δ_{max} in ENOC4 is a result of good rubber-filler interaction.

There is another interesting phenomenon in the room temperature region. The tan δ is much lower in this region in the case of ENOC4 when compared with EN and ENUN4, though the storage modulus is higher in the case of ENOC4 than those of EN and ENUN4.

CONCLUSIONS

1. The clay, NaMMT, has been modified by octadecyl amine. The amine chain is intercalated between the layers of the clay, and has been verified by XRD and FTIR. The 2θ peak in XRD is shifted toward the lower value, in the 3–10° range, indicating an increase in the gallery gap. The characteristic peaks for the amine appeared in the FTIR spectra of the modified clay, supporting the intercalation of the amine into the UN layers.
2. The Engage-clay nanocomposites have been prepared and characterized by XRD, FTIR, and TEM.
3. The X-ray diffractograms show an increase in the gallery gap with the intercalation of the polymer chains into the clay galleries. The unmodified clay is highly intercalated, while the modified clay gets exfoliated. The FTIR spectra show characteristic peaks of both the clay and the polymer, signifying the presence of clay in the nanocomposites. The TEM on the other hand shows agglomeration of the unmodified clay particles in the rubber matrix. But the modified clay particles are partially exfoliated with an average thickness of ~13 nm.
4. The addition of the modified clay to the polymer displays distinct improvement in tensile strength, modulus, and elongation at break compared to the gum or the unmodified clay-filled nanocomposite. The tensile strength increases with filler loading, and optimizes at 4 phr loading.
5. Increased T_g in the nanocomposite indicates better polymer-filler interaction in the composite. In the rubbery region, the storage modulus of ENOC4 is higher than those of EN and ENUN4.

TABLE V
Dynamic Mechanical Properties of Nanocomposites

Sample name	T_g (°C)	tan δ at T_g	tan δ at 25°C	log E' at 25°C (MPa)	log E' at 70°C (MPa)
EN	−55	0.33	0.18	6.05	5.87
ENUN4	−55	0.33	0.18	6.31	5.96
ENOC4	−45	0.31	0.07	6.93	5.97

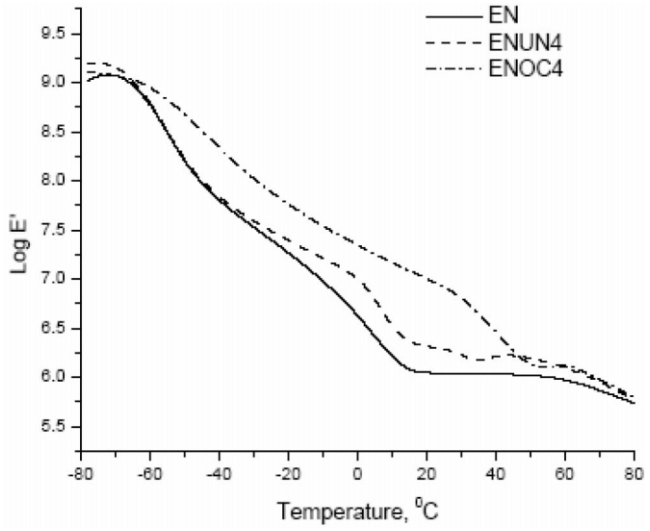

(a)

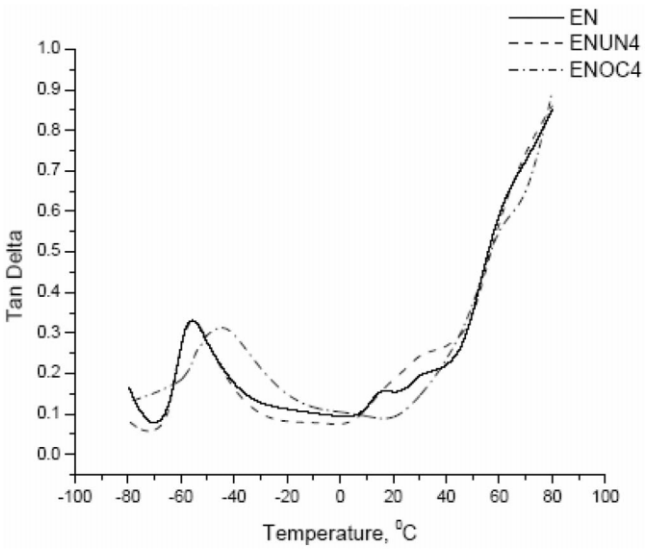

(b)

Figure 5 (a) Plot of storage modulus versus temperature; (b) Plot of tan δ versus temperature.

References

1. Giannelis, E. P.; Krishnamoorti, R.; Manias, E. In Advances in Polymer Science 1998, 138, 107.
2. Vaia, R. A.; Giannelis, E. P. Macromolecules 1997, 30, 7990.
3. Lan, T.; Kaviratna, P. D.; Pinnavaia, T. J. Chem Mater 1995, 7, 2144.
4. Lyatskaya, Y.; Balazs, A. C. Macromolecules 1998, 31, 6676.
5. Kojima, Y.; Usuki, A.; Kawasumi, M.; Fukushima, Y.; Okada, A.; Kurauchi, T.; Kamigaito, O. J Mater Res 1993, 8, 1185.
6. Kojima, Y.; Usuki, A.; Kawasumi, M.; Okada, A.; Kurauchi, T.; Kamigaito, O. J Polym Sci Part A: Polym Chem 1993, 31, 983.
7. Lepoittevin, B.; Devalckenaere, M.; Pantoustier, N.; Alexandre, M.; Kubies, D.; Calberg, C.; Jerome, R.; Henrist, C.; Cloots, R.; Dubois, P. Polymer 2002, 43, 4017.

8. Usaki, A.; Koiwai, A.; Kojima, Y.; Kawasumi, M.; Okada, A.; Kurauchi, T.; Kamigaito, O. J Appl Polym Sci 1995, 55, 119.
9. Shelley, J. S.; Mather, P. T.; DeVries, K. L. Polymer 2001, 42, 5849.
10. Agag, T.; Takeichi, T. Polymer 2001, 42, 3399.
11. Lincon, D. M.; Vaia, R. A.; Wang, Z. G.; Hsiao, B. S. Polymer 2001, 42, 1621.
12. Kim, G. M.; Lee, D. H.; Hoffmann, B.; Kressler, J.; Stoppelmann, G. Polymer 2001, 42, 1095.
13. Cho, J. W.; Paul, D. R. Polymer 2001, 42, 1083.
14. Fornes, T. D.; Yoon, P. J.; Keskkula, H.; Paul, D. R. Polymer 2001, 42, 9929.
15. Rayneud, E.; Jouen, T.; Ganthier, C.; Vigier, G.; Varlet, J. Polymer 2001, 42, 8759.
16. Hambir, S.; Bulakh, N.; Kodgire, P.; Kalgaonkar, R.; Jog, J. P. J Polym Sci Part B: Polym Phys 2001, 39, 446.
17. Ma, J.; Qi, Z.; Hu, Y. J Appl Polym Sci 2001, 82, 3611.
18. Kawasumi, M.; Hasegawa, N.; Kato, M.; Usuki, A.; Okada, A. Macromolecules 1997, 30, 6333.
19. Godgire, P.; Kalgaonkar, R.; Hambir, S.; Bulakh, N.; Jog, J. P. J Appl Polym Sci 2001, 81, 1786.
20. García-López, D.; Picazo, O.; Merino, J. C.; Pastor, J. M. Eur Polym J 2003, 39, 945.
21. Alexandre, M.; Dubois, P.; Sun, T.; Graces, J. M.; Jerome, R. Polymer 2002, 43, 2123.
22. Vu, Y. T.; Mark, E. J.; Pham, L. H.; Engelhardt, M. J Appl Polym Sci 2001, 82, 1391.
23. Pramanik, M.; Srivastava, S. K.; Samantaray, B. K.; Bhowmick, A. K. J Polym Sci Part B: Polym Phys 2002, 40, 2065.
24. Dietsche, F.; Thomann, Y.; Thomann, R.; Mulhaupt, R. J Appl Polym Sci 2000, 75, 396.
25. Kornmann, X.; Lindmerg, H.; Berglund, L. A. Polymer 2001,42, 4493.
26. Wang, Z.; Pinnavaia, T. J. Chem Mater 1998, 12, 3769.
27. Sadhu, S.; Bhowmick, A. K. Rubber Chem Technol 2003, 76, 860.
28. Sadhu, S.; Bhowmick, A. K. J Appl Polym Sci 2004, 92, 698.
29. Sadhu, S.; Bhowmick, A. K. J Polym Sci Part B: Polym Phys 2004, 42, 1573.
30. www.dupont-dow.com (accessed January 23, 2004).
31. Ray, S.; Bhowmick, A. K. J Appl Polym Sci 2002, 83, 2255.
32. Jha, A.; Bhowmick, A. K. Rubber Chem Technol 1997, 70, 798.